and in system 2 the four minima (l,l,l), (l,l,r), (l,r,r), and (r,r,r). If the electrical field changes from large positive to large negative values, the dipole moment of the hydrogen bond changes in system 1 from +6 to -6 D and in system 2 from +10 to -10 D. In the case of system 1 this field-dependent change is largest at $\pm 0.6 \times 10^7$ V/cm and in system 2 if no field is present. Thus, if electrical fields of this size are present at the hydrogen-bonded system, their proton polarizability is largest. At 300 K it amounts to 200×10^{-24} cm^3 (system 1) and 500×10^{-24} cm^3 (system 2), i.e., it increases with increasing length of the hydrogen-bonded chains. Thus, the proton polarizability of such hydrogen-bonded chains is more than 2 orders of magnitude larger than the polarizablity caused by distortion of electron systems. As in the case of single hydrogen bonds, the energy levels shift strongly as a function of the electrical field strength. Furthermore, as characteristic for potentials with more than one minimum, a large number of transitions is observed. They shift as a function of the electrical field strength. Some vanish, some arise.

As consequence of all these results such chains are particularly suitable for the proton conduction in biological systems. According to the results presented here the hydrogen-bonded chain postulated in the case of bacteriorhodopsin[6,7] would show very large proton polarizability. The same should be true in the case of all hydrogen-bonded chains that have been already studied experimentally with model systems.[6-10]

Acknowledgment. We thank the Deutsche Forschungsgemeinschaft for providing the facilities for this work.

Registry No. HCO_2H, 64-18-6; H_2O, 7732-18-5; HCO_2^-, 71-47-6; H^+, 12408-02-5.

Kinetics of the Thermal Dehydration of Potassium Copper(II) Chloride Dihydrate

Haruhiko Tanaka* and Nobuyoshi Koga

Chemistry Laboratory, Faculty of School Education, Hiroshima University, Shinonome, Minami-Ku, Hiroshima, 734, Japan *(Received: October 15, 1987)*

Thermogravimetry (TG) complemented by differential scanning calorimetry (DSC) has been used to study the kinetics of the dehydration of powdered and single-crystal samples of $K_2CuCl_4 \cdot 2H_2O$. The dehydration of single crystals was followed by observing, microscopically in polarized light, thin sections of the sample dehydrated to different fractions reacted, α. The mass-change traces for the isothermal dehydration of the powdered material were recorded at different temperatures. Nonisothermal dehydration of single crystals proceeds in three stages: (1) surface nucleation and growth of nuclei, followed by the advancement of reaction fronts inward, (2) random nucleation and growth near the reaction front as well as in the bulk, and (3) the rapid escape of water vapor through the cracks formed by crystallization of the solid product in the bulk. The isothermal dehydration of the powdered material, which proceeded in a single step, was described by a contracting geometry law, $1 - (1 - \alpha)^{1/n} = kt$, with $1 < n < 2$. Under nonisothermal conditions, the single-step dehydration could also be described by a contracting geometry model with the exponent n being slightly different from that in the isothermal analysis. This was substantiated by a comparison of the rate constants, k, derived isothermally with those calculated in terms of the kinetic compensation effect for nonisothermal dehydration at various heating rates.

Introduction

It is well-known that the thermal decomposition of those solids which yield solid and gaseous products proceeds in a very complex way.[1] The process consists of several stages, e.g., the chemical act of breaking of bonds, followed by destruction of the reactant crystal lattice, formation of nuclei of the solid product and growth of these nuclei, adsorption-desorption of gaseous products, diffusion of gases, and heat transfer.[2] It is possible that the decomposition mechanism changes during the course of reaction, that is, a kinetic model $F(\alpha)$, which describes the kinetic law of a reaction, sometimes varies depending on the fraction reacted α. Moreover, in some cases, the decomposition kinetics are described not only by a single mechanism but by a combination of different mechanisms.[3,4] Since there is still some ambiguity in many kinetic results from conventional thermal analyses, further methods are required to clarify the kinetics of solid-state decompositions. Along with conventional thermoanalytical methods, complementary physicochemical techniques, e.g., electron microscopy[5] and X-ray diffractometry[6] are necessary for a better understanding of such complicated kinetics.[7] It was also reported that polarizing microscopy of thin sections is useful for determining the decomposition mechanisms of single crystals.[8-10]

In the present study, the dehydration of powdered and single-crystal samples of $K_2CuCl_4 \cdot 2H_2O$ has been singled out, because preliminary TG-DSC runs show that single crystals dehydrate in a very complicated way, while the dehydration behavior of the powdered material is apparently quite simple. Moreover, the powdered material dehydrates quantitatively to the anhydride at lower temperatures and in a narrower temperature region than the single crystals, without formation of any stable intermediate hydrate. It was also hoped that polarizing microscopy would be as valuable as other techniques, e.g., scanning electron microscopy and X-ray diffractometry, in determining the dehydration mechanism of single crystals.

Experimental Section

Single crystals of potassium copper(II) chloride dihydrate were prepared from a supersaturated solution of $CuCl_2 \cdot 2H_2O$ (Katayama Chemical Co.; reagent grade) and KCl mixed in a molar ratio of 1:2 at room temperature. The powdered material was obtained by grinding the single crystals with a mortar and pestle, and -100+170, -48+100, and +48 mesh sieve fractions were collected. The sample was characterized by IR spectroscopy as well as TG. About 30 mg of the single crystals were loaded onto a platinum pan of 5-mm diameter and 2.5-mm height in a Rigaku Thermoflex TG-DSC 8085 E1 system. TG-DSC traces were recorded simultaneously at a linear heating rate of 1.85 °C/min in N_2 flowing through a reactor of 15-mm diameter at a rate of

(1) Brown, M. E.; Dollimore, D.; Galwey, A. K. *Reactions in the Solid State*; Elsevier: Amsterdam, 1980; Chapter 4.
(2) Zsako, J. *J. Phys. Chem.* **1968**, *72*, 2406.
(3) Johnson, D. W.; Gallagher, P. K. *J. Phys. Chem.* **1971**, *75*, 1179.
(4) Ball, M. C.; Norwood, L. S. *J. Chem. Soc. A* **1968**, 1633.
(5) Galwey, A. K. *Thermal Analysis*; Wiley Heydon: Chichester, U.K., 1982; Vol. 1, pp 38-53.
(6) Beer, H. R.; Oswald, H. R. *Thermal Analysis*; Birkhaeuser: Basel, 1980; Vol. 2, pp 121-127.
(7) Sestak, J.; Berggren, G. *Thermochim. Acta* **1971**, *3*, 1.
(8) Tanaka, H.; Yabuta, Y.; Koga, N. *React. Solids* **1986**, *2*, 169.
(9) Tanaka, H.; Kawabata, K. *Thermochim. Acta* **1985**, *92*, 219.
(10) Brown, M. E. *Thermochim. Acta* **1987**, *110*, 153.

0022-3654/88/2092-7023$01.50/0

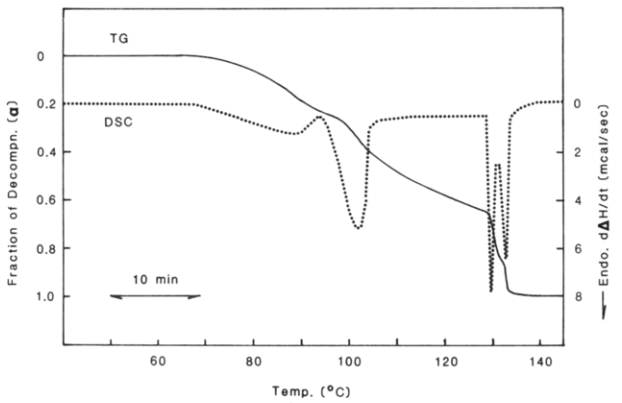

Figure 1. Typical simultaneous TG–DSC traces for the nonisothermal dehydration of single crystals of $K_2CuCl_4 \cdot 2H_2O$.

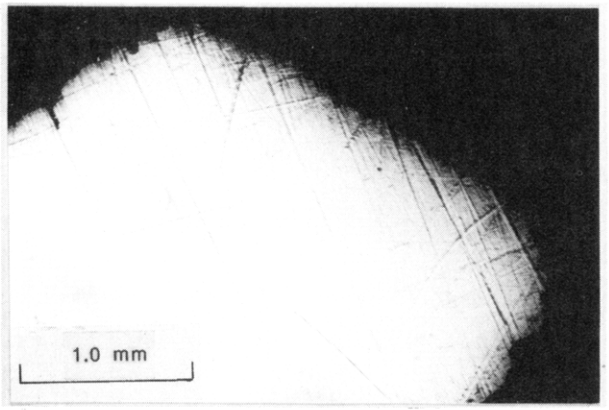

Figure 2. Typical polarizing microscopic view of the (100) face of a thin section of an unreacted single crystal of $K_2CuCl_4 \cdot 2H_2O$.

30 mL/min. Ignited Al_2O_3 was used as reference material. Simultaneous TG–DSC curves at various heating rates were also obtained for ca. 20-mg samples of the powder. The mass-change traces for the isothermal dehydration of the powdered material were recorded at different temperatures under conditions similar to those for dynamic runs.

Thin sections (ca. 0.03-mm thickness) of single crystals dehydrated to different fractions reacted, α, were prepared as described elsewhere[8,9] and observed with a polarizing microscope and photographed. In addition, a half-dehydrated powder sample of a +48 mesh sieve fraction was observed in transmitted light after it had been embedded in an adhesive resin and the top had been abraded with abrasive cloth and paper as well as abrasive powder (Corundum no. 1500).

The data obtained from thermogravimetry were processed by using a microcomputer with plotter. The linearity of an appropriate plot was assessed by means of the correlation coefficient γ and/or the standard deviation σ of linear regression analyses to determine the best kinetic model and the kinetic parameters. The uncertainties of these kinetic parameters are given in terms of the standard deviations.

Results and Discussion

Single Crystals. Figure 1 shows typical simultaneous TG–DSC traces for the nonisothermal dehydration of single crystals of $K_2CuCl_4 \cdot 2H_2O$ to K_2CuCl_4. We see from Figure 1 that dehydration proceeds in three approximately separate stages I, II, and III. It was observed from microscopic studies that stage I began with rapid nucleation on the surface and growth of nuclei inward, which resulted in the advancement of the reaction front. That is, the dehydration proceeds according to a contracting geometry model, R_n. Figures 2 and 3 are typical microscopic views of the (100) face of unreacted and 20%-dehydrated crystals, respectively. Figure 2 shows that the reactant material is uniformly single crystalline and optically homogeneous. We see from Figure 3 that the product layer and the reaction front are not necessarily

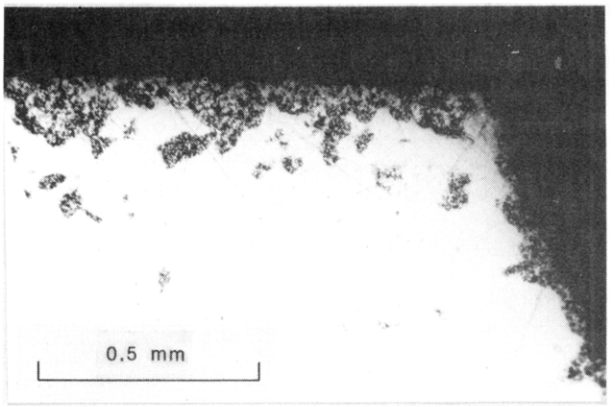

Figure 3. Typical polarizing microscopic view of the (100) face of a thin section of a 20%-dehydrated single crystal of $K_2CuCl_4 \cdot 2H_2O$.

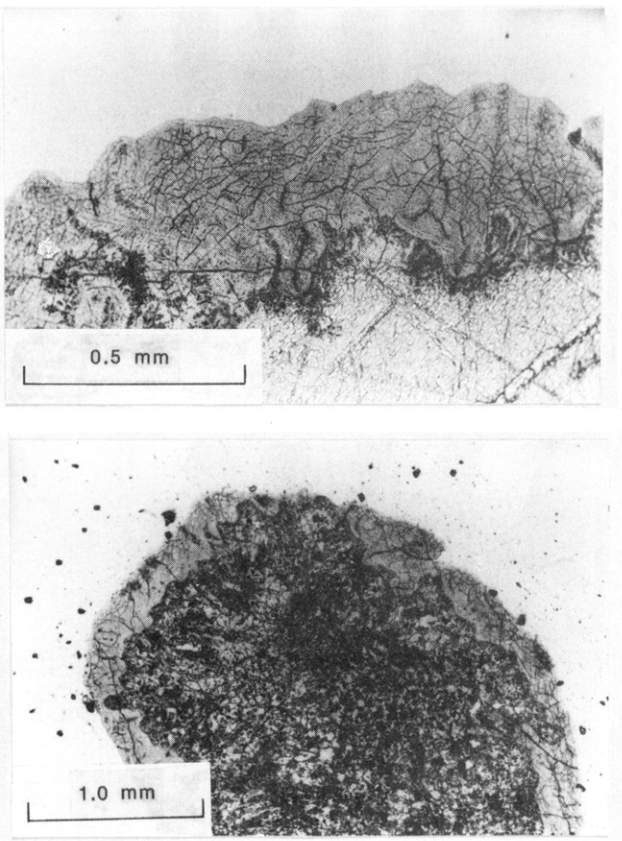

Figure 4. Polarizing microscopic view of the (100) face of thin sections of a (top) 50%- and (bottom) 70%-dehydrated single crystal of $K_2CuCl_4 \cdot 2H_2O$.

uniform. We note that there is no nucleation in the bulk at this stage, although some nucleation and growth occur near the reaction front.

In the early stage of II, there is a rapid increase in the rate of heat absorption with fairly rapid loss in mass. In the later stage, however, the rate of heat absorption decreases slightly with nearly constant loss in mass. The slope of the TG curve at this stage as a whole is likely to suggest a reaction controlled by a mechanism of random nucleation and subsequent growth, A_m, in the bulk. The nearly constant rate of heat absorption in the later stage of II might result from the exothermic crystal growth of product and endothermic liberation of water. Such speculations can be substantiated by examining thin sections of the 50%- and 70%-dehydrated materials, which are shown in the top and bottom panels of Figure 4, respectively.

It is noted in Figure 4 (top) that cracks in the product layer were produced by some volume contraction due to the dehydration. It is interesting to note that the layers of product of the early stage of II contain needlelike crystals, which in turn provide passages

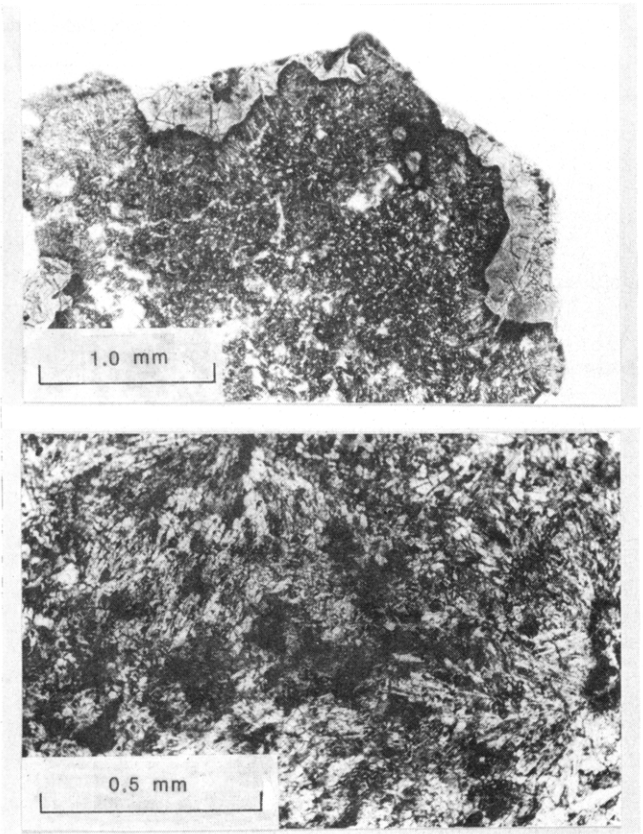

Figure 5. Polarizing microscopic view of the (100) face of a thin section of the end product of dehydration of $K_2CuCl_4 \cdot 2H_2O$.

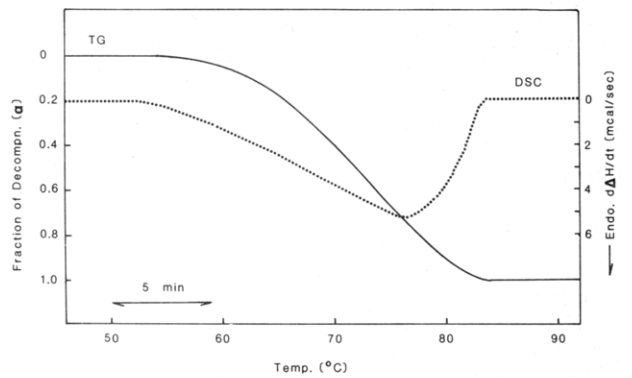

Figure 6. Simultaneous TG–DSC traces for the nonisothermal dehydration of powdered $K_2CuCl_4 \cdot 2H_2O$ (−100+170 mesh) at a heating rate of 1.80 °C/min.

for the evolved water vapor to diffuse outward. The formation of needlelike crystals seems to be catalyzed by a higher vapor pressure of the water evolved in the bulk,[8,11,12] since it is likely that such crystals grew in the opposite direction to diffusion of the water vapor. We see from Figure 4 (bottom) that the product crystallizes also in the bulk in the later stage of II.

For stage III, the rapid loss in mass in Figure 1 is clearly due to liberation of water through the cracks in the sample produced during the later stage of II. The tail of the TG curve may arise from slow desorption and diffusion of water vapor and from the reverse reaction. Figure 5 shows a thin section of the end product. We can recognize needlelike crystals of the product in the bulk, which were produced at stage III. The rapid regression of DSC trace to the base line at this stage seems to correspond to the exothermic crystal growth of the product.

(11) Garner, W. E. In *Chemistry of the Solid State*; Garner, W. E., Ed.; Butterworths: London, 1955; Chapter 8.
(12) Young, D. A. *Decomposition of Solids*; Pergamon: Oxford, 1966; Chapter 3.

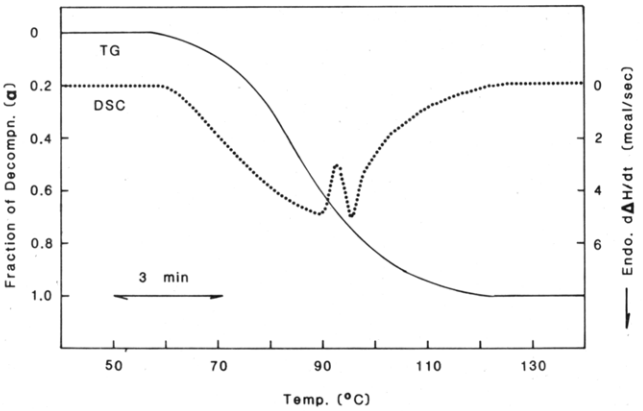

Figure 7. Simultaneous TG–DSC traces for the nonisothermal dehydration of the powdered $K_2CuCl_4 \cdot 2H_2O$ (−100+170 mesh) at a heating rate of 6.93 °C/min.

TABLE I: Kinetic Model Functions, $F(\alpha)$

model	$F(\alpha)$	label
Avrami–Erofeyev	$[-\ln(1-\alpha)]^{1/m}$, $m = 1, 2, 3, 4$	A_m
contracting geometry	$1-(1-\alpha)^{1/n}$, $n = 1, 2, 3$	R_n
Prout–Tompkins	$\ln[\alpha/(1-\alpha)]$	A_u
one-dimensional diffusion	α^2	D_1
two-dimensional diffusion	$\alpha + (1-\alpha)\ln(1-\alpha)$	D_2
Jander	$[1-(1-\alpha)^{1/3}]^2$	D_3
Ginstling–Broushtein	$1-2\alpha/3-(1-\alpha)^{2/3}$	D_4

Powdered Material. Figure 6 shows the simultaneous TG–DSC traces for the dehydration of the powdered material under conditions similar to those for the single crystals. Figure 7 shows typical TG–DSC traces recorded for the dehydration of powdered $K_2CuCl_4 \cdot 2H_2O$ at a higher heating rate of 6.93 °C/min. No splitting of the DSC peak was observed at heating rates lower than 3.40 °C/min. It is worth determining the kinetic model function $F(\alpha)$[7] and Arrhenius parameters for the dehydration of powdered $K_2CuCl_4 \cdot 2H_2O$ under both isothermal and nonisothermal conditions, in terms of the respective temperature, T, and the time, t, as a function of the fraction dehydrated, α. It is reasonable here to evaluate the kinetics at lower heating rates in the case of nonisothermal dehydrations, in view of correspondence with the isothermal condition and of an undesired change in the simple TG–DSC curves into the complicated at higher heating rates.

(*a*) *Analyses in the Range $0.1 \leq \alpha \leq 0.9$.* Table I shows kinetic model functions, $F(\alpha)$, examined in the present study. Table II shows a typical result of linear regression analysis of $F(\alpha)$ vs t plots for the isothermal dehydration of powdered $K_2CuCl_4 \cdot 2H_2O$ (−100+170 mesh), assuming kinetic equations $F(\alpha) = kt$, where k is the rate constant. Table III shows the probable functions $F(\alpha)$ and Arrhenius parameters estimated for the isothermal dehydration of samples of different particle sizes. It is difficult at present to provide a clear explanation of the nonintegral values, m and n, in A_m and R_n, but these values were adopted merely to obtain better linearity in the $F(\alpha)$ vs t plot,[13] the physical meaning of which will be discussed later. We have been conscious of the shortcoming that the temperature interval examined in the isothermal runs is too narrow. This resulted from a requirement of assuring the trace of dehydration in a range $0.1 \leq \alpha \leq 0.9$ at a reasonably constant temperature (±0.1 °C). It seems, in view of the correlation coefficient γ of linear regression analysis of the Arrhenius plot and the standard deviations σ of E and log A, that the present analysis is not necessarily meaningless. On the contrary, in the light of undesired possible changes in the sample condition due to a temperature effect,[4] the present results seem to be useful for a better understanding of kinetics of isothermal solid-state reactions.

Although it is difficult to single out the correct $F(\alpha)$ for the present isothermal dehydration, the effect of particle size on the rate constant k is likely to serve the purpose. Table IV shows the

(13) Ng, W.-L. *Aust. J. Chem.* **1975**, *28*, 1169.

TABLE II: Rate Constants k from Linear Regression Analysis of Plots of Probable $F(\alpha)$ Function vs Time t for a Typical Isothermal Dehydration of $K_2CuCl_4 \cdot 2H_2O$[a]

	$R_{1.45\pm0.03}$			$A_{2.11\pm0.03}$		
temp, °C	k, 1/s	γ[b]	σ[c]	k, 1/s	γ[b]	σ[c]
50.7	1.7976×10^{-4}	0.9996	6.38×10^{-3}	2.6656×10^{-4}	0.9995	1.03×10^{-2}
52.6	2.7470×10^{-4}	0.9994	7.66×10^{-3}	4.0732×10^{-4}	0.9993	1.28×10^{-2}
54.5	3.4852×10^{-4}	0.9997	5.96×10^{-3}	5.1672×10^{-4}	0.9994	1.17×10^{-2}
55.0	3.7511×10^{-4}	0.9998	4.00×10^{-3}	5.5602×10^{-4}	0.9994	1.19×10^{-2}
57.4	4.9887×10^{-4}	0.9996	5.99×10^{-3}	7.3955×10^{-4}	0.9993	1.27×10^{-2}

[a] For a particle-size fraction of −100+170 mesh. [b] Correlation coefficient of linear regression analysis of $F(\alpha)$ vs t plots. [c] Standard deviation of each point from the line.

TABLE III: Appropriate Function, $F(\alpha)$, Activation Energy, E, and Preexponential Factor, A, for the Isothermal Dehydration of $K_2CuCl_4 \cdot 2H_2O$ for Varying Particle-Size Fractions[a]

particle-size fraction, mesh	temp range, °C	$F(\alpha)$	E, kJ/mol	log A, 1/s	$-\gamma$[b]
−100+170	50.7–57.4	$R_{1.45}$	133 ● 5	17.7 ● 0.8	0.9918
		$A_{2.11}$	133 ● 5	17.9 ± 0.7	0.9919
−48+100	53.5–58.3	$R_{1.67}$	126 ± 5	16.4 ± 0.8	0.9870
		$A_{1.90}$	126 ± 4	16.6 ● 0.6	0.9868
+48	53.4–58.5	$R_{1.86}$	121 ± 7	15.4 ● 1.1	0.9907
		$A_{1.69}$	121 ± 4	15.7 ● 0.7	0.9905

[a] Analyzed in a range $0.1 \leq \alpha \leq 0.9$. [b] Correlation coefficient of the linear regression analysis of the Arrhenius plot.

TABLE IV: Particle-Size Effect on the Rate Constant, k, Derived Isothermally

particle-size fraction, mesh	$F(\alpha)$[a]	k,[b] 1/s
−100+170	$R_{1.47}$	3.30×10^{-4}
−48+100	$R_{1.72}$	2.06×10^{-4}
+48	$R_{1.76}$	1.52×10^{-4}

[a] Appropriate kinetic model function derived from $F(\alpha)$ vs t plots. [b] Values at 54.5 °C.

particle-size effect on the value of n in the R_n reaction model and k. It seems, at least qualitatively, that the isothermal dehydration of powdered samples is regulated by an R_n law because the k values decrease with increasing particle size.[14] At present, it is almost impossible to discuss this relation quantitatively as the value n in the R_n model is changing as well as k.

The nonisothermal dehydration of powdered samples was analyzed according to the Ozawa[15,16] and the Coats and Redfern (CR)[17,18] methods. Table V shows probable models $F(\alpha)$, assessed from plots of $F(\alpha)$ vs the generalized time θ,[15,16] and the kinetic parameters derived from the Ozawa method for the nonisothermal dehydrations at various heating rates.[19] We may assume that the contracting geometry models, R_n, describe the nonisothermal dehydration of crystalline powders of $K_2CuCl_4 \cdot 2H_2O$, although the A_m laws are not necessarily inappropriate in view of the γ value.

Results from the CR method, in terms of the $F(\alpha)$ functions estimated isothermally, are shown in Table VI for the dehydration of powdered samples of −100+170, −48+100, and +48 mesh, respectively. We see from Table VI that A_m gives a better fit than R_n, contrary to the results from the isothermal and the Ozawa methods. It seems that the above discrepancy is due to combination of A_m and R_n laws[4] as well as change in the mechanism during the course of dehydration, which make the situation very complicated. The combined model suggested above can be substantiated by observing partially dehydrated powders of $K_2CuCl_4 \cdot 2H_2O$ with a microscope. Figure 8 shows typical micrographs, observed in transmitted light, of an internal surface of a +48 mesh sample which was half-dehydrated. We see that there is combination of the A_m and R_n models. It is noted here that the fraction

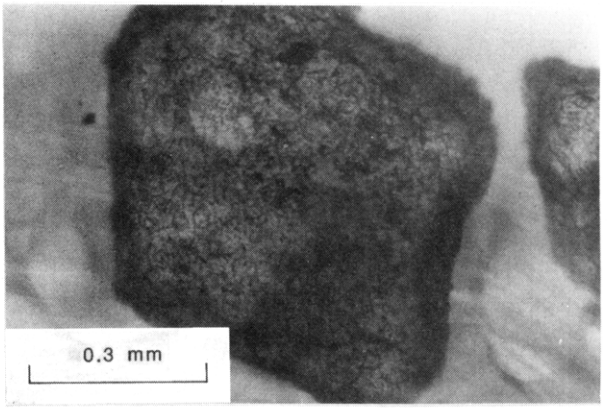

Figure 8. Typical microscopic view, in transmitted light, of an inside plane of a half-dehydrated sample of a +48 mesh sieve fraction of $K_2CuCl_4 \cdot 2H_2O$.

dehydrated, α, was not always 0.5 for the particles, because the relation, $\alpha = 0.5$, according to TG, means 50% mass loss on an average over all the particles in a pan. It is clear that this is one of the reasons for the present feature of the dehydration of powdered material. The nonintegral values of n and m derived mathematically might be explained in connection with the reaction model combined.

Recently it was suggested that a "true" kinetic compensation effect,[20,21] found for nonisothermal decompositions of solids at various heating rates, is useful for checking the $F(\alpha)$ function estimated conventionally against that found isothermally.[22] According to this, it is interesting to compare the k values derived isothermally with those calculated in terms of the kinetic compensation equation $\log A = a + bE$, where a and b are constants. Table VII shows the k values derived isothermally and from the compensation law, assuming the $F(\alpha)$ functions estimated isothermally, for the dehydration of powdered $K_2CuCl_4 \cdot 2H_2O$ of different particle sizes. We see in view of the correspondence of the k values that, although R_n is not necessarily to be ruled out, A_m is slightly better than R_n but not as good in comparison with instances reported earlier.[22] This seems to be ascribed to the fact that the dehydration is controlled not by a single mechansim but by combination of two or more laws, e.g., R_n and A_m, as deduced

(14) Hulbert, S. F. *J. Br. Ceram. Soc.* **1969**, *6*, 11.
(15) Ozawa, T. *Bull. Chem. Soc. Jpn.* **1965**, *38*, 1881.
(16) Ozawa, T. *J. Therm. Anal.* **1970**, *2*, 301.
(17) Coats, A. W.; Redfern, J. P. *Nature (London)* **1964**, *201*, 68.
(18) Zsako, J. *J. Therm. Anal.* **1973**, *5*, 239.
(19) Koga, N.; Tanaka, H. *J. Therm. Anal.* **1988**, *34*, 177.
(20) Sestak, J. *Thermophysical Properties of Solids; Their Measurements and Theoretical Thermal Analysis*; Elsevier: Amsterdam, 1984; Chapters 8 and 9.
(21) Nikolaev, A. V.; Logvinenko, V. A. *J. Therm. Anal.* **1976**, *10*, 363.
(22) Tanaka, H.; Koga, N. *J. Therm. Anal.* **1987**, *32*, 1521.

TABLE V: Appropriate Function, $F(\alpha)$, and Kinetic Parameters Derived from the Ozawa Method for the Nonisothermal Dehyration of $K_2CuCl_4 \cdot 2H_2O$ for Varying Particle-Size Fractions[a]

particle-size fraction, mesh	$F(\alpha)$	E,[b] kJ/mol	log A, 1/s	$-\gamma$[c]	σ[d]
−100+170	$R_{3.33}$	124 ± 3	15.7 ± 0.1	0.999 95	0.132×10^{-2}
	$A_{1.33}$	124 ± 3	16.2 ± 0.1	0.999 70	1.21×10^{-2}
−48+100	$R_{2.33}$	103 ± 2	12.5 ± 0.2	0.999 95	0.178×10^{-2}
	$A_{1.54}$	103 ± 2	12.9 ± 0.3	0.999 42	1.48×10^{-2}
+48	$R_{2.44}$	98.4 ± 1.4	11.7 ± 0.2	0.999 97	0.138×10^{-2}
	$A_{1.48}$	98.4 ± 1.4	12.1 ± 0.3	0.999 58	1.29×10^{-2}

[a] Analyzed in a range $0.1 \leq \alpha \leq 0.9$. [b] Averaged over a range $0.1 \leq \alpha \leq 0.9$. [c] Correlation coefficient of linear regression analysis of $F(\alpha)$ vs θ plot. [d] Standard deviation of each point from the line.

TABLE VI: Kinetic Parameters Derived from the CR Method, in Terms of $F(\alpha)$ Estimated Isothermally, for the Nonisothermal Dehydrations of $K_2CuCl_4 \cdot 2H_2O$ for −100+170, −48+100, and +48 Mesh Sieve Fractions[a]

particle-size fraction, mesh	heating rate, °C/min	$F(\alpha)$ = R_n[b] E, kJ/mol	log A, 1/s	$-\gamma$[d]	$F(\alpha)$ = A_m[c] E, kJ/mol	log A, 1/s	$-\gamma$[d]
−100+170	0.482	189	26.2	0.9930	111	14.2	1.0000
	0.914	163	22.0	0.9896	95.3	11.8	0.9992
	1.803	132	17.1	0.9846	76.8	8.93	0.9972
	3.258	123	15.7	0.9905	70.8	8.14	0.9990
−48+100	0.480	163	22.1	0.9928	104	13.1	0.9980
	0.972	137	17.8	0.9894	87.5	10.5	0.9974
	1.852	124	15.9	0.9912	79.1	9.27	0.9978
	3.279	120	15.1	0.9931	75.2	8.68	0.9990
+48	0.504	160	21.5	0.9884	112	14.4	0.9961
	0.961	132	17.0	0.9918	92.0	11.2	0.9978
	1.820	114	14.1	0.9947	79.0	9.18	0.9987
	3.403	118	14.7	0.9934	82.1	9.66	0.9991

[a] Analyzed in a range $0.1 \leq \alpha \leq 0.9$. [b] $n = 1.45$, 1.67, and 1.86 for particle-size-fraction ranges of −100+170, −48+100, and +48, respectively. [c] $m = 2.11$, 1.90, and 1.69 for particle-size-fraction ranges of −100+170, −48+100, and +48, respectively. [d] Correlation coefficient of the linear regression analysis of the CR plot.

TABLE VII: Comparison of the Rate Constants, k, Derived Isothermally with Those Calculated in Terms of the Compensation Effect for the Nonisothermal Dehydration of $K_2CuCl_4 \cdot 2H_2O$ at Different Heating Rates

particle-size fraction, mesh	$F(\alpha)$	k,[a] 1/s isothermally	k,[a] 1/s from compensation law[b]	compensation const[c] $-a$	b	γ[d]
−100+170	$R_{1.45}$	3.51×10^{-4}	1.34×10^{-4}	4.016	0.160	0.9999
	$A_{2.11}$	5.23×10^{-4}	2.96×10^{-4}	2.962	0.155	0.9999
−48+100	$R_{1.67}$	2.23×10^{-4}	1.17×10^{-4}	4.133	0.161	0.9999
	$A_{1.90}$	3.79×10^{-4}	2.64×10^{-4}	2.964	0.154	0.9998
+48	$R_{1.86}$	1.58×10^{-4}	1.05×10^{-4}	3.921	0.159	1.0000
	$A_{1.69}$	3.30×10^{-4}	2.53×10^{-4}	3.076	0.155	1.0000

[a] Value at 55.0 °C. [b] Calculated using the values of log A derived isothermally in terms of each $F(\alpha)$. [c] For the equation $\log A = a + bE$. [d] Correlation coefficient of the linear regression analysis of compensation plot.

TABLE VIII: Appropriate Function, $F(\alpha)$, and Kinetic Parameters for the Isothermal Dehydration of $K_2CuCl_4 \cdot 2H_2O$ for Varying Particle-Size Fractions[a]

particle-size fraction, mesh	temp range, °C	$F(\alpha)$	E, kJ/mol	log A, 1/s	$-\gamma$[b]
−100+170	50.7–57.4	$R_{1.47}$	131 ± 5	17.4 ± 0.7	0.9923
		$A_{2.41}$	131 ± 5	17.5 ± 0.8	0.9924
−48+100	53.5–58.5	$R_{1.72}$	131 ± 6	17.2 ± 0.9	0.9837
		$A_{2.01}$	131 ± 6	17.4 ± 0.9	0.9841
+48	53.4–58.5	$R_{1.76}$	118 ± 6	15.0 ± 0.9	0.9891
		$A_{1.94}$	118 ± 4	15.2 ± 0.6	0.9889

[a] Analyzed in a range $0.3 \leq \alpha \leq 0.8$. [b] Correlation coefficient of the linear regression analysis of the Arrhenius plot.

from the direct observation of an internal surface of partially dehydrated material. We speculate, in addition, that the "weighting" of the two laws varies between the isothermal and nonisothermal dehydrations. That is, under isothermal conditions, the R_n law may dominate the mechanism to a larger extent than under nonisothermal conditions. It is interesting to recall that the Ozawa method yields the activation energy E at a given fraction dehydrated, α, although only values averaged over a range $0.1 \leq \alpha \leq 0.9$ were given in Table V. Figure 9 shows the activation energy E at various α from 0.1 to 0.9 in steps of 0.05 for the dehydration of powdered materials of various particle sizes. E decreases with increasing α, particularly at smaller α. This may imply that the mechanism of the dehydration changes as the reaction proceeds, as has been illustrated above in the case of the single-crystal material. Accordingly, it seems worthwhile examining the kinetics of dehydration of powdered $K_2CuCl_4 \cdot 2H_2O$ in a restricted range $0.3 \leq \alpha \leq 0.8$ and comparing the results with those for the range $0.1 \leq \alpha \leq 0.9$.

(*b*) *Analyses in the Range* $0.3 \leq \alpha \leq 0.8$. Table VIII lists the Arrhenius parameters for the isothermal dehydration of $K_2CuCl_4 \cdot 2H_2O$ powders of various particle sizes. Practically identical $F(\alpha)$ and kinetic parameters are derived for analyses in both the ranges $0.3 \leq \alpha \leq 0.8$ and $0.1 \leq \alpha \leq 0.9$. Slight differences in $F(\alpha)$ and kinetic parameters between the two α ranges suggest that the "weighting" of the two or more mechanistic laws combined varies depending on α. It is likely that this variation is considerable in a range at smaller α, e.g., $0.1 < \alpha < 0.3$. Table IX lists the kinetic model function $F(\alpha)$ and kinetic parameters derived from

TABLE IX: Appropriate Function, $F(\alpha)$, and Kinetic Parameters Derived from the Ozawa Method for the Nonisothermal Dehydration of $K_2CuCl_4 \cdot 2H_2O$ for Varying Particle-Size Fractions[a]

particle-size fraction, mesh	$F(\alpha)$	E,[b] kJ/mol	log A, 1/s	$-\gamma$[c]	σ[d]
−100+170	$R_{3.85}$	119 ± 2	14.9 ± 0.1	0.9999	1.10×10^{-3}
	$A_{1.30}$	119 ± 2	13.2 ± 0.1	0.9999	4.88×10^{-3}
−48+100	$R_{2.08}$	100 ± 1	12.1 ± 0.1	0.9998	2.22×10^{-3}
	$A_{1.72}$	100 ± 1	12.4 ± 0.1	0.9999	2.40×10^{-3}
+48	$R_{2.13}$	96.0 ± 0.8	11.4 ± 0.1	0.9999	1.56×10^{-3}
	$A_{1.69}$	96.0 ± 0.8	11.7 ± 0.1	0.9999	3.48×10^{-3}

[a] Analyzed in a range $0.3 \leq \alpha \leq 0.8$. [b] Averaged over a range $0.3 \leq \alpha \leq 0.8$. [c] Correlation coefficient of linear regression analysis of $F(\alpha)$ vs θ plot. [d] Standard deviation of each point from the line.

TABLE X: Kinetic Parameters Derived from the CR Method, in Terms of $F(\alpha)$ Estimated Isothermally, for the Nonisothermal Dehydrations of $K_2CuCl_4 \cdot 2H_2O$ for −100+170, −48+100, and +48 Mesh Sieve Fractions[a]

particle-size fraction, mesh	heating rate, °C/min	$F(\alpha)$					
		R_n[b]			A_m[c]		
		E, kJ/mol	log A, 1/s	$-\gamma$[d]	E, kJ/mol	log A, 1/s	$-\gamma$[d]
−100+170	0.482	165	22.5	0.9901	89.8	10.9	0.9901
	0.914	142	18.8	0.9939	76.8	8.91	0.9979
	1.804	115	14.5	0.9946	61.8	6.62	0.9988
	3.260	111	14.0	0.9966	59.5	6.40	0.9981
−48+100	0.480	141	18.7	0.9928	89.1	10.8	0.9915
	0.972	120	15.2	0.9983	75.5	8.62	0.9986
	1.852	111	13.8	0.9993	69.6	7.78	0.9999
	3.279	110	13.6	0.9987	69.0	7.73	0.9991
+48	0.504	137	18.0	0.9944	89.5	10.8	0.9949
	0.961	115	14.4	0.9971	74.5	8.45	0.9982
	1.820	100	12.0	0.9968	64.5	6.95	0.9977
	3.403	107	13.1	0.9966	69.6	7.79	0.9982

[a] Analyzed in a range $0.3 \leq \alpha \leq 0.8$. [b] $n = 1.47$, 1.72, and 1.76 for particle-size-fraction ranges of −100+170, −48+100, and +48, respectively. [c] $m = 2.41$, 2.01, and 1.94 for particle-size-fraction ranges of −100+170, −48+100, and +48, respectively. [d] Correlation coefficient of the linear regression analysis of the CR plot.

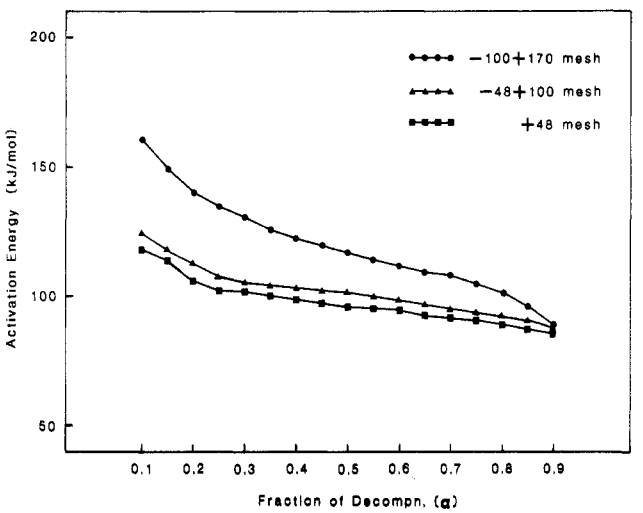

Figure 9. Activation energies, E, at various fractions reacted, α, derived from the Ozawa method for the nonisothermal dehydration of powdered $K_2CuCl_4 \cdot 2H_2O$ at different heating rates.

the Ozawa method for the nonisothermal dehydrations of powdered $K_2CuCl_4 \cdot 2H_2O$ of various particle sizes. Table X shows the parameters derived from the CR method, in terms of the $F(\alpha)$ functions estimated isothermally, for the same nonisothermal runs.

For the nonisothermal dehydrations, although the $F(\alpha)$ functions are nearly identical, the kinetic parameters derived in a range $0.3 \leq \alpha \leq 0.8$ are a little smaller than those in a range $0.1 \leq \alpha \leq 0.9$. This difference in the kinetic parameters between the two ranges is clearly due to the higher values of E at smaller α values, i.e., in a range $0.1 \leq \alpha \leq 0.3$ (see Figure 9).

Kinetic Comparison between the Powdered and Single-Crystalline Materials. We see, by comparing Figure 1 with Figure 6, that TG–DSC curves for the powdered material are very smooth and that the powdered material is much more labile kinetically than the single-crystal material. This is probably due to less influence by the self-generated water vapor pressure, less blocking action by the solid product layer, and so on. These effects will be diminished by a decrease in particle size. The larger the particle size, the more separate were the DSC peaks. The extreme case of the appearance of separate peaks is seen in the dehydration of the single-crystal material (see Figure 1).

The DSC peaks also separate at higher heating rates for a given range of particle size. This fact implies that the sample conditions, e.g., temperature, thermal agitation, and vapor pressure of self-generated water in the bulk, are influenced by the heating rate, which in turn may change the kinetic model. This is one of the reasons why it is appropriate to record TG–DSC traces at lower heating rates, as in the present study, particularly in relating the data to the isothermal analysis.[23] Although dehydration behaviors are very different between the powdered and single-crystalline materials, it is important that the information from the latter serves to elucidate the kinetics of the former.

Conclusions

The nonisothermal dehydration of single crystals of $K_2CuCl_4 \cdot 2H_2O$ proceeds mainly in three distinct stages. They correspond to (1) surface nucleation and growth of these nuclei followed by advancement of reaction fronts inward, (2) random nucleation and growth (Avrami–Erofeyev law, A_m) near the reaction front and in the bulk, and (3) the rapid escape of water vapor following the recrystallization of product in the bulk.

A systematic kinetic analysis of the dehydration of the powdered material revealed the following: (1) Under isothermal conditions, it is dehydrated according to a contracting geometry model, R_n, with the exponent $1 < n < 2$. (2) The kinetic models of the nonisothermal dehydration, of the powdered material, which proceeds much faster than that for the single-crystal material, were estimated as R_n and A_m according to Ozawa and CR methods, respectively. (3) On the whole, the R_n law was assumed to describe the isothermal and nonisothermal dehydrations of the powdered material, though it is more or less combined with other

(23) Tanaka, H.; Ohshima, S.; Ichiba, S.; Negita, H. *Thermochim. Acta* **1981**, *48*, 137.

models which include A_m as well as R_n with different values of n.

It is likely that the simpler behavior of the dehydration of powdered material, as can be seen from TG and DSC traces, compared with that of single-crystal material is explained by (1) the decreased influence of the vapor pressure of self-generated water and less blocking action by the solid product layer and (2) the fact that the TG and DSC traces due to the dehydration of the former are based on the average over a great number of particles, whereas that of the latter is specific to the material with anisotropy.

Acknowledgment. We thank Professor G. Yoshino for his help in observing thin sections in polarized light and taking the photographs.

Registry No. $K_2CuCl_4 \cdot 2H_2O$, 10085-76-4.

Formation of Highly Oriented Graphite from Poly(acrylonitrile) Prepared between the Lamellae of Montmorillonite

Naohiro Sonobe, Takashi Kyotani, Yoshihiro Hishiyama,† Minoru Shiraishi,‡ and Akira Tomita*

Chemical Research Institute of Non-Aqueous Solutions, Tohoku University, Katahira 2-1-1, Sendai, Japan 980 *(Received: December 23, 1987)*

An attempt was made to prepare a carbon sample having a highly oriented structure from poly(acrylonitrile) by using a two-dimensional opening between the lamellae of montmorillonite as the field of carbonization. The carbon prepared at 700 °C was liberated from montmorillonite and then it was subjected to heat treatment at various temperatures up to 2800 °C. The characteristics of the resulting carbon were determined by microscopic, diffractometric, spectroscopic, and magnetoresistance methods. The graphitizability of the carbon is very high, and the carbon heat-treated at 2800 °C has almost the same characteristics as the ideal graphite crystal. It consists of graphitic films with L_c value of about 40 nm and very large L_a value of more than 1 μm in many cases. The reason for such a high graphitizability was ascribed to the formation of a two-dimensional carbon precursor in the early stages of carbonization.

Introduction

Highly oriented two-dimensional graphite is expected to have various interesting physical properties such as high conductivity, optical anisotropy, and high radiation resistance, and, therefore, can be applied as a new material in the fields of advanced technology. At present, HOPG[1] (highly oriented pyrolytic graphite) and kish graphite[2] have been known as artificial graphite of high crystallinity. However, severe conditions (3500 °C, 25 MPa) are required to prepare HOPG.

Recently, Ohnishi et al.[3] and Murakami et al.[4] reported that highly oriented graphite films can be prepared from special kinds of polymers. However, no one has attempted to prepare a graphite film from a conventional polymer such as poly(acrylonitrile) (PAN) by designing the carbonization procedure.

In a previous paper,[5] we reported the preparation of carbon from PAN at 700 °C by using a two-dimensional opening between the lamellae of montmorillonite, with the expectation to produce a two-dimensional carbon. The obtained carbon was liberated from montmorillonite and characterized by various methods.[5] This preparation method and the graphitization process of this carbon have been briefly reported in a short communication.[6] We report here the graphitization process and the characteristics of the resultant carbon in more detail. The carbons heat-treated at various temperatures from 1000 to 2800 °C were characterized by scanning and transmission electron microscopies, X-ray and electron diffraction, Raman scattering, and magnetoresistance effect. As a reference, a carbon prepared from an ordinary PAN was heat-treated and characterized as well.

Experimental Section

Preparation of Carbons. Two powdery carbons prepared in the previous study were used as starting materials. One is that prepared by using the space between the lamellae of montmorillonite, and another one is a carbon from a conventional PAN. They were termed IPC and FPC, which mean the carbon derived from intercalated polymer and free polymer, respectively.

TABLE I: Elemental Analyses of Heat-Treated Carbons (wt %)

sample	C	H	N	O(diff)
IPC	66	3	16	15
IPC10	84	0	10	6
IPC12	90	0	4	6
IPC14	96	0	2	2
IPC16	99	0	1	0
FPC	73	1	19	7
FPC10	91	0	9	0
FPC12	96	0	3	1
FPC14	98	0	1	1
FPC16	99	0	1	0

IPC and FPC were subjected to heat treatment at temperatures up to 2800 °C, using an electric furnace with a carbon heater under N_2 or Ar flow. The temperature was raised at a heating rate of 10 °C/min to a predetermined temperature and held there for 1 h. The heat-treatment temperature (HTT) is indicated in this paper by the number following IPC or FPC. For example, IPC28 refers to an IPC heat-treated at 2800 °C. For the magnetoresistance measurements, carbon powder was first pelletized and then heat-treated as above. The pellet is stable even after heat treatment.

Characterization of Carbons. The interplanar spacing and the crystallite size of the carbon were determined with an X-ray diffractometer (Shimadzu, VD-1) which was calibrated with a silicon standard. Generally, a standard powder diffraction method

† Musashi Institute of Technology, Tamazutsumi 1-28-1, Setagaya, Tokyo, Japan 158.
‡ National Research Institute for Pollution and Resources, Onogawa 16-3, Tsukuba, Japan 305.

(1) Moore, A. W. In *Chemistry and Physics of Carbon*; Walker, Jr., P. L., Thrower, P. A., Eds., Dekker: New York, 1973; Vol. 11, p 69.
(2) Austerman, S. B. In *Chemistry and Physics of Carbon*; Walker, Jr., P. L., Thrower, P. A., Eds., Dekker: New York, 1968; Vol. 4, p 137.
(3) Ohnishi, T.; Murase, I.; Noguchi, T.; Hirooka, M. *Synth. Met.* **1986**, *14*, 207.
(4) Murakami, M.; Watanabe, K.; Yoshimura, S. *Appl. Phys. Lett.* **1986**, *48*, 1594.
(5) Sonobe, N.; Kyotani, T.; Tomita, A. *Carbon* **1988**, *26*, 573.
(6) Kyotani, T.; Sonobe, N.; Tomita, A. *Nature (London)* **1988**, *331*, 331.

0022-3654/88/2092-7029$01.50/0